Chemical Engineering Journal 145 (2008) 232–241

Contents lists available at ScienceDirect

Chemical Engineering Journal

journal homepage: www.elsevier.com/locate/cej

On the contribution of the scales of mixing to the oxygen transfer in stirred tanks

Mariano Martín*, Francisco J. Montes, Miguel A. Galán

Departamento de Ingeniería Química y Textil, Universidad de Salamanca Pza, de los Caídos 1-5, 37008 Salamanca, Spain

ARTICLE INFO

Article history:
Received 23 January 2008
Received in revised form 13 April 2008
Accepted 15 April 2008

Keywords:
Macromixing
Micromixing
Mixing time
Turbulence
Mass transfer
Stirred tanks

ABSTRACT

Two main scales of mixing can be considered inside a stirred tank: macromixing and micromixing. Macromixing is related to the tank size circulation and is responsible for bubble motion, surface aeration and tank homogenization. Meanwhile, micromixing is related to the small liquid eddies, responsible for the concentration gradients surrounding the bubbles, and it prevails around the impeller. Experimental results and empirical equations are used and proposed to unveil the contribution of both mechanisms to the volumetric mass transfer coefficient, k_La. A model has been proposed to predict a mean k_La as a combination of both mechanisms. In case of consumption of oxygen due to chemical reactions, micromixing plays a dominant role. However, only by considering the macromixing contribution to the total k_La is it possible to explain the scale up problems traditionally reported for stirred tanks due to the important effect that the hydrodynamics plays: removal of the superficial air liquid contact, baffles, stirrer type, etc.

1. Introduction

Mass transfer from a gas phase dispersed into a liquid phase is a widely spread phenomenon in chemical engineering in order to provide several components to the liquid phase. Inside contact equipment, the dispersion of the gas phase is achieved by means of spargers and/or using impellers.

Inside a stirred tank different scales of mixing are present, and there are regions where one of the scales of mixing prevails, macromixing or micromixing. Many studies have been accomplished to unveil those regions using different techniques, studying chemical reactions taking place in a stirred tank and the dispersion of concentration in the tank, namely, the intensity of segregation [1–17].

Micromixing prevails near the impeller, where small eddies define the velocity gradients surrounding the bubbles. Since, according to Kolmogorov's theory, the power per unit volume determines the energy and size of the eddies, it has traditionally been used in the design and scale up of equipment [3,7–9,11,14].

Macromixing prevails surrounding the micromixing region. It determines the internal homogenization, the movement of bubbles across the reactor and the flow pattern in which the turbulent eddies are tank-sized. Then, the contribution of the surface aeration of a tank as well as the effect of the geometry of the impeller and the tank to the mass transfer depend on this scale of mixing [1,3,7–10].

Since in a multiphase reactor, the mass transfer rate between phases depends on the concentration gradients surrounding the bubbles [6,11,18], on the liquid mixing in the tank [1,14–17,19], and on the kinetics of the reaction, consequently, both scales of mixing must be considered.

The contribution of each scale depends on the internal geometric configuration of the tank. It is widely accepted that stirring and gas flow rate improve the macromixing in the tank. However, this fact does not guarantee an improvement in micromixing, which can be achieved by feeding the reactant close to the impeller [1,14,17].

Theoretical equations for predicting the volumetric mass transfer coefficient, k_La, are traditionally based on the study of the turbulent eddies surrounding the bubbles using the isotropic turbulence theory of Kolmogorov [20,21]. Precisely, Kolmogorov's theory models micromixing.

However, this theory does not consider the dispersed phase and its effect on the mixing. The gas phase not only modifies the power input, [22,23], but it can also reduce the effective contact area if the dispersion generated is not appropriately scattered, [24], increasing the mixing time, [25]. Moreover, tank geometry and scale up affect the empirical coefficient k of the empirical equations for the design of stirred tanks [26]. As a result, the study of liquid turbulence cannot entirely explain the mass transport phenomenon because it is focused on the eddies, without considering the gas phase.

Another effect to be considered in the modellization of multiphase systems is the case of chemical reactions taking place in the

* Corresponding author. Tel.: +34 923294479; fax: +34 923294574.
E-mail address: mariano.m3@usal.es (M. Martín).

1385-8947/$ – see front matter © 2008 Elsevier B.V. All rights reserved.
doi:10.1016/j.cej.2008.04.019

Nomenclature

a	specific area (m^{-1})
B	number of blades of the turbine
D	tank diameter (m)
D_o	orifice diameter (m)
D_{ab}	diffusivity (m^2 s)
g	gravity ($m\,s^{-2}$)
h	position of the impeller over the plate (m)
H_f	reactor height (m)
J	width of the baffles (m)
k, K	constants
k_L	mass transfer coefficient in the liquid phase ($m\,s^{-1}$)
k_La	volumetric mass transfer coefficient (s^{-1})
K_{sensor}	sensor constant (s^{-1})
L	length of the blades (m)
n	number of turbines
N	impeller speed (s^{-1})
P_{o1}	individual power number
P_o	power number
P	power input (W)
P_g	aerated power input (W)
Q_c	gas flow rate ($m^3\,s^{-1}$)
R	number of baffles in the reactor
t	time (s)
T	impeller diameter (m)
T_i	width of the blade (m)
u	velocity of turbulence ($m\,s^{-1}$)
u_G	superficial gas velocity ($m\,s^{-1}$)
U_∞	rising velocity of the bubble ($m\,s^{-1}$)
V	tank volume (m^3)
W	width of the blade (m)

Greek symbols

α and β	empirical coefficients with respect to the power input and the gas flow rate respectively
χ	fraction of the tank where the macromixing prevails
ε	power input per unit mass ($W\,kg^{-1}$)
η	length of turbulence (m)
μ	dynamic viscosity (Pa s)
ν	kinematic viscosity ($m^2\,s^{-1}$)
ρ	liquid density ($kg\,m^{-3}$)
θ	mixing time (s)
σ	surface tension (N m)

liquid bulk consuming the dissolved gas. Thus, there is an increment in the effective k_La [25]. Several equations have been proposed to predict the enhancement factor as function of the kinetics of the reaction [28,29]. This factor multiplies the effects of the variables that determine the liquid film resistance such as the physical properties of the phases, the transport properties, etc., and so k_La.

Therefore, the aim of this work is to explain the effect of the impeller type, dispersion device and configuration and scale up on k_La, based on the contribution of the mixing scales present in the tank. In order to do so, different single impellers have been used to evaluate the contribution of both scales as a result of the particular flow pattern developed by each one and their effect on the bubbles. Furthermore, combinations of two or three impellers in standard laboratory scale or pilot plant bioreactors have also been considered to study the effect of different geometrical configurations on the contribution of both scales of mixing as well as on the effect of scale up. These configurations are the most efficient for gas–liquid contact [26]. To explain the contribution of both scales to k_La, an expression for k_L in macromixing conditions as well as a model to predict the mean k_La as function of the regions of the tank where one of the scales of mixing prevails has been proposed based on the models of network of zones used by many authors, Funahashi, Nienow, Alves, Mann [1,5,6,8,12–17,30–36].

2. Theoretical considerations

Based on the available theories and models for mass transfer rates in stirred tanks, due to Funahashi et al. [1], Kawase and Moo-Young [20] and Barabash and Belevitskaya [37], an expression for the liquid film resistance has been proposed in order to account for the effect of the movement of the bubbles across the tank as well as the contribution of the surface aeration which are related to the macromixing scale. Kawase's equation is used to determine the contribution of the micromixing to the total k_La.

2.1. Micromixing contact time

The effect of the turbulent eddies developed by the flow on the velocity profiles and thus on the concentration profiles surrounding the bubbles can be studied through Higbie's theory [38].

Higbie's theory provides an expression for the liquid film coefficient. According to it, k_L depends on the turbulence intensity expressed as dissipated energy as long as the surface removal is quicker than in the case of bubbles rising under potential flow, Eq. (1)

$$k_L = \frac{2}{\sqrt{\pi}}\sqrt{\frac{D_{ab}}{t}} \tag{1}$$

Kawase and Moo-Young [20] proposed that the contact time between phases, t, could be considered as the ratio between the length of turbulence (η) and the turbulent velocity (u) defined by the Kolmogorov's theory of isotropic turbulence. Both magnitudes characterize the turbulent flow developed in the stirred tank.

$$\eta = \left(\frac{\nu^3}{\varepsilon}\right)^{1/4} \tag{2}$$

$$u = (\nu\varepsilon)^{1/4} \tag{3}$$

The input power per unit mass is considered as that given by the impeller. For a Newtonian medium, the expression obtained is Eq. (4), [20]:

$$k_L = \frac{2}{\sqrt{\pi}}\sqrt{D_{ab}}\left(\frac{\varepsilon\rho}{\mu}\right)^{1/4} \tag{4}$$

In order to predict k_La, not only the liquid phase resistance to the mass transfer is needed, but also the contact area between phases. The specific area is calculated using the empirical equation of Calderbank [39].

$$a = 1.44\left[\frac{(P_g/V)^{0.4}\rho^{0.2}}{\sigma^{0.6}}\right]\left(\frac{u_G}{U_\infty}\right)^{0.5} \tag{5}$$

2.2. Macromixing contact time

Inside a stirred tank, the presence of an impeller generates a pattern of energy dissipated which leads to different mechanisms of mass transfer [1,3,5,6,11]. As a result, the bubbles have no constant exposition time, as Dankwerts had proposed [39]. Therefore, not only the micromixing scale exposed by Kawase and Moo-Young [20] has its contribution to k_La, but also the macromixing.

The contribution of macromixing to k_La was proposed by Funahashi et al. [1] accounting for the fact that the region near

the impeller is governed by the micromixing scale, meanwhile macromixing prevails surrounding the micromixing region.

Furthermore, one of the most unpredictable problems in scale up is the effect of the geometry of the impeller, the baffles, etc. on the mass transfer rate. This effect is related to the macromixing. The flow pattern developed in the tank depends on the geometry of each tank and impeller and is responsible for bubble motion and for the contribution of the superficial aeration. Bubbles can be dragged throughout the tank following the flow pattern developed inside due to the impeller. During this movement, the liquid phase surrounding the bubble changes, which can be somehow quantified by the mixing time [1]. This consideration resembles the one for bubble columns in which the contact time is the time a bubble takes to move along its diameter [38]. Additionally, the tank size vortexes are responsible for the renewal of the gas–liquid surface.

So, in Higbie's theory, instead of using the turbulent contact time given by the isotropic turbulence, the contact time will be considered as the mixing time. It is proposed that k_L be written as follows:

$$k_L = \frac{2}{\sqrt{\pi}}\sqrt{\frac{D_{ab}}{\theta}} \tag{6}$$

The mixing time is a well known concept. However, there is no theoretical equation to calculate it due to geometrical difficulties. Nevertheless, several well tested equations with theoretical basis (turbulence theory) and experimentally verified are available, like the one proposed by Nienow [19].

$$\theta = 5.9\left(\frac{T}{D}\right)^{-1/3}\varepsilon^{-1/3}D^{2/3} \tag{7}$$

Although the equation has been obtained for one single impeller in non aerated conditions, it is claimed that can be used for aerated systems by correcting the power input [40–42]. Therefore, the unaerated power input must be modified to take into account the effect of the gas on the impeller by equations like the one given by Hugmark [22]:

$$\frac{P_g}{P} = 0.1\left(\frac{N^2T^4}{gWV^{2/3}}\right)^{-1/5}\left(\frac{Q_c}{NV}\right)^{-1/4} \tag{8}$$

Furthermore, in the case of working with multiple impellers, not only the same power relationship between the mixing time and the power input has experimentally been found as in Eq. (7) [43,44] but also Cooke et al. [45] found a similar expression as Eq. (7) for dual impeller systems. Others pointed out that Eq. (7) provides the minimum mixing time [46] for systems with multiple impellers.

In general, the effect of the multiple impellers is the reduction in the amount of zoning in the tank [47]. Thus, more complex equations for predicting the mixing time for multiple impellers have been proposed in the literature to account for the geometrical characteristics of the tank and the position of the impellers [48]. However, the number of adjustable parameters, up to six, and the theoretical basis of Nienow's equation backs its use. More accurate models of the contribution of both scales can be obtained using CFD methods to determine the macro and the micromixing times in further studies.

2.3. Other effects on the volumetric mass transfer coefficient

The consumption of oxygen in the bulk mass by a chemical reaction modifies the mass transfer resistance in the liquid side. In order to cope with this effect, an enhancement factor has traditionally been proposed. This factor depends on the kinetics of the reaction. Several authors have developed theoretical expressions for this factor depending on the working system [28,29]. The measured k_La includes this effect.

The differences in the surface tension near the interphase, due to the mass transfer, also modify the contact time [49,50]. As a result, the mass transfer is enhanced by convective motion, which modifies the velocities at the interphase. But, at the same time, the convective motion is limited by the macroscopic flow inside the tank [51]. This also supports the fact that both scales of mixing must be considered.

3. Experimental method

3.1. Experimental setup

3.1.1. Pilot plant reactor

A pilot plant scale bioreactor, BIOSTAT C® was used to determine k_La in a standard geometry for the air–water system. The geometrical characteristics of the reactor can be seen in Table 1.

The power number for Rushton turbines is calculated using the equation proposed by Richards [52]:

$$P_{o1} = 336.5\left(\frac{W}{D}\right)\left(\frac{L}{D}\right)^{1.5}\left(\frac{J}{D}\right)^{0.3}\left(\frac{B}{6}\right)^{0.56}\left(\frac{R}{4}\right)^{0.4} \tag{9}$$

Since the separation between turbines yields between 1.5 and 2 times the turbine diameter, the total power number can be calculated using [52]:

$$P_o = nP_{o1} \tag{10}$$

where n is the number of turbines. The total unaerated power can be calculated using Eq. (11):

$$P = P_o\rho N^3T^5 \tag{11}$$

The control loop of the BIOSTAT C® was fixed in order to work at 20 °C with deionized water (ρ = 998 kg/m^3, σ = 0.073 N/m, $\mu = 1.037\times10^{-3}$ Pa s).

One of the most important problems in chemical engineering is scale up. In the case of stirred tanks, it is known that using constant power input at laboratory and industrial size, the impeller speed decreases while scaling up. So, in order to evaluate the contribution of the different scales of mixing on k_La during the scale up of a process, low rotational speeds are used, from 50 to 200 min^{-1}. The flow rates have been used from 1.5×10^{-5} m^3/s to 1×10^{-4} m^3/s.

Furthermore, in this way, the experimental range of impeller speeds used by other authors [26] is widened.

In addition, Table 2 shows the coefficients obtained by fitting the experimental values of k_La to Eq. (12) for the air–water system by Linek et al. [53] and Arjunwadkar et al. [54]

$$k_La = k\left(\frac{P_g}{V}\right)^{\alpha}u_G^{\beta} \tag{12}$$

Table 1
Geometrical characteristics of BIOSTAT C®

Volume (L)	D (m)	H_f (m)	T (m)	Baffles	J (m)	Turbines	Blades/Turbine	L (m)	W (m)	W_{Baffle} (m)	D_o (m)
20	0.21	0.44	0.084	4	0.02	3	6	0.024	0.017	0.014	0.001

Table 2
Empirical equations and characteristics

	k	α	β	Operation conditions	Impeller	P_o*
[53]	4.95×10^{-3}	0.593	0.4	D = 0.29 m, u_G: 2.12–4.24 mm/s, N = 4.17–14.17 rps	Rushton 6 blades	5
[54]	2.04×10^{-3}	0.68	0.58	D = 0.18 m, u_G: 0.98–3.3 mm/s, N = 6.6–12.5 rps	Disk turbine, pitched blade turbine	5 + 1.27

*[61,62].

that will also be used in this study to compare the effect of different configurations on the contribution of the macro and micromixing scales.

3.1.2. Non standard tank

In order to determine the effect of the position of the impellers and that of the impeller geometry on the governing scale of mixing, the data from a previous work Martin et al. [24] were used. The tank used for obtaining them consisted of a prism of a 15 cm × 15 cm × 15 cm laser sealed made of glass. A gas chamber is located in the base of the tank 5 cm × 5 cm × 5 cm divided into two with a top chamber 2 cm × 2 cm × 2 cm in which the dispersion device was fixed. The first dispersion device is a one-holed perforated plate of 2 mm of diameter, the other, instead of one orifice, it has two orifices, each of 2 mm of diameter, with a separation between both of 6 mm in order to avoid coalescence.

Deionized water (20 °C, $\rho = 998\ \text{kg/m}^3$, $\sigma = 0.073\ \text{N/m}$, $\mu = 1.037 \times 10^{-3}\ \text{Pa s}$), was desoxygenated by means of a nitrogen flow rate. Three different air flow rates were used for each dispersion device, $0.6 \times 10^{-6}\ \text{m}^3/\text{s}$, $1.4 \times 10^{-6}\ \text{m}^3/\text{s}$ and $2.8 \times 10^{-6}\ \text{m}^3/\text{s}$ for the one-holed dispersion device and, $0.3 \times 10^{-6}\ \text{m}^3/\text{s}$, $0.6 \times 10^{-6}\ \text{m}^3/\text{s}$ and $1.4 \times 10^{-6}\ \text{m}^3/\text{s}$ due to setup limitations for the dispersion device with two holes. Bigger gas flow rates overwhelmed the seal of the gas chambers.

Five different impellers, standard ones like a Rushton turbine or a propeller, and non standard ones, like different pitched blade turbines or a modified blade, were located at 3 vertical positions (0.02 m, 0.035 m and 0.05 m). Furthermore, 2-bladed, 3-bladed at 120° and 4-bladed impellers, were used to study the effect of the number of blades on the mass transfer rate. Their diameter is 6 cm and the height of the blades is 0.7 cm. The one-hole dispersion device and $h = 0.02$ m were used, along with gas flow rates of $0.6 \times 10^{-6}\ \text{m}^3/\text{s}$, $1.4 \times 10^{-6}\ \text{m}^3/\text{s}$ and $2.8 \times 10^{-6}\ \text{m}^3/\text{s}$, and the same rotational speeds as exposed above.

Three rotational speeds, 180 rpm, 280 rpm and 430 rpm were used for all these impellers.

The liquid working volume consists of the volume of the whole tank up to 8 cm above the dispersion device. The effect of the gas phase on the liquid surface represents the effect of the volume of gas inside a closed stirred tank. Further description of the impellers, their power numbers, etc. can be found in the same previous work [24].

3.2. Electrode response time

k_La is measured using the dynamic method which avoids the use of surfactants responsible for modifying the coalescence behaviour of the system. The only problem can be the response time of the electrode.

Therefore, a two resistance model was used to model the electrode, taking into consideration the resistance of the membrane of the electrode. The model can be seen elsewhere [55–57]. The experimental value for K_{sensor} is $0.230\ \text{s}^{-1}$.

4. Results and discussion

First, the effect of the geometry of the impellers and the tank, and the gas flow rate on the contribution of macro and micromixing scales to k_La was evaluated for a system with no consumption of oxygen in the liquid phase, the air–water system. Then, the consumption of oxygen by the media on the prevailing mass transfer mechanism was evaluated.

In order to study the effect of the gas phase on the mass transfer mechanism, k_La is going to be plotted versus the ratio P/V. So that, for a known P, with the power number of the impeller configuration, it is possible to determine the rotational speed needed for the calculation of P_g/P in Eq. (5). Thus, k_La can be calculated through empirical equations.

In the case of the air–water system, without consumption of oxygen by the media, Fig. 1 shows the comparison of the effect of both mechanisms on the mass transfer for the systems used by Linek et al. [53] and Arjunwadkar et al. [54]. For low gas flow rates, the main mass transfer mechanism depends on the configuration of the reactor and the impellers used. The impeller configuration determines the fraction of the tank where either macro or micromixing prevails. However, the empirical values from both authors come close to each other with the increment in the superficial gas velocity. This can be explained based on the fact that the increment in the gas flow rate favors the mixing inside the tank [14,17]. Furthermore, the empirical results are always within the predicted values in case of the macromixing or the micromixing.

Now that the effect of geometry on the contribution of both scales of mixing to k_La has been proved, the effect of the scale up on the prevailing scale is going to be analyzed. The experimental results obtained in the BIOSTAT C® for the air–water system were correlated to Eq. (13).

$$k_La = 0.001\left(\frac{P_g}{V}\right)^{0.37}(u_G)^{0.54} \tag{13}$$

The comparison between the experimental values of k_La and the calculated ones using Eq. (13) can be seen in Fig. 2. Good agreement is shown.

If a figure based on the same principles as Fig. 1 is developed, Fig. 3, it can be seen that the dominant mechanism is macromixing. The low turbulence and the small effect of the impeller on the bubbles due to the low rotational speed do not allow a high bubble break up. The deformability of the bubbles, mainly due to the macroscopic flow inside the tank, is the main mass transfer mechanism since it is responsible for the contact area and for the concentration profiles surrounding the bubbles. Therefore, it can be concluded that if scale up is not made carefully, the mass transfer rate in the tank can decrease.

The effect of different configurations on the contribution of the micro and macromixing to k_La is based on the different flow patterns developed by the impellers as well as the interactions between impellers. Therefore, to explain the effect of the geometry of the impellers on the contribution of the scales of mixing and the effect of bubble size, giving a deeper knowledge of the phenomena, the experimental results of Martin et al. [58] for the eight types of the impellers (pitched blades turbines, modified blades, Rushton

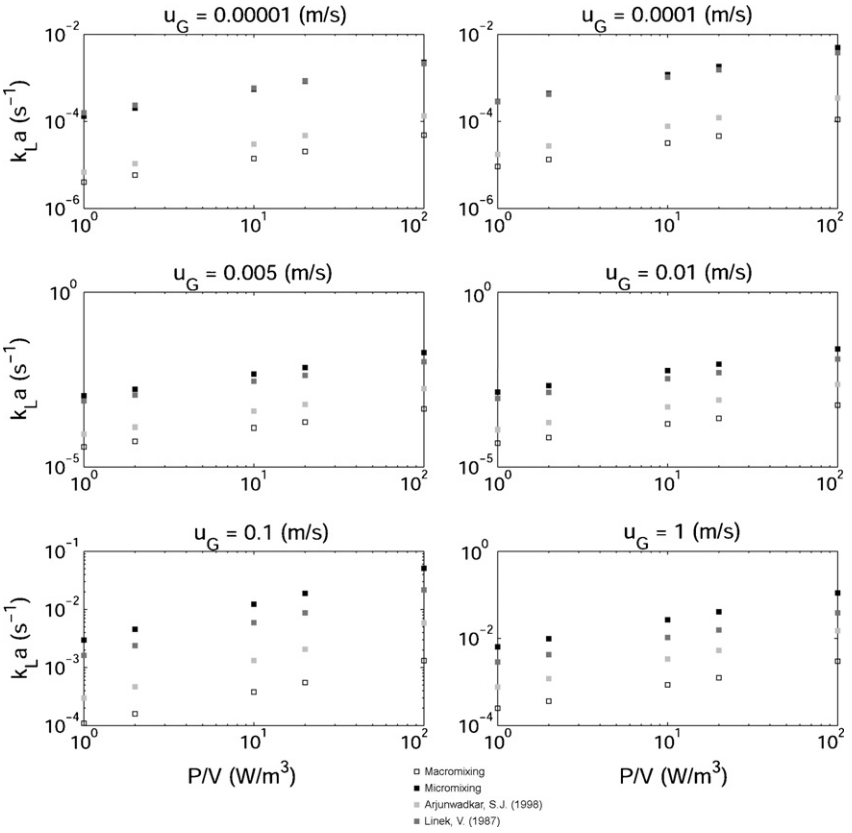

Fig. 1. Macro and micromixing effects on mass transfer.

turbine, propeller and 2-, 3- and 4-bladed turbines), are going to be used.

Figures like Figs. 1 and 3 are prepared for all the impellers and dispersion devices under consideration [58], the effect of both scales of mixing can be studied. Figs. 4 and 5 plot the experimental k_La for just two of the impellers, the Rushton turbine and the propeller, versus power input including k_La calculated using Eq. (4) (micromixing) and Eq. (6) (macromixing) for different gas flow rates and dispersion devices (one-holed and two-holed perforated plates).

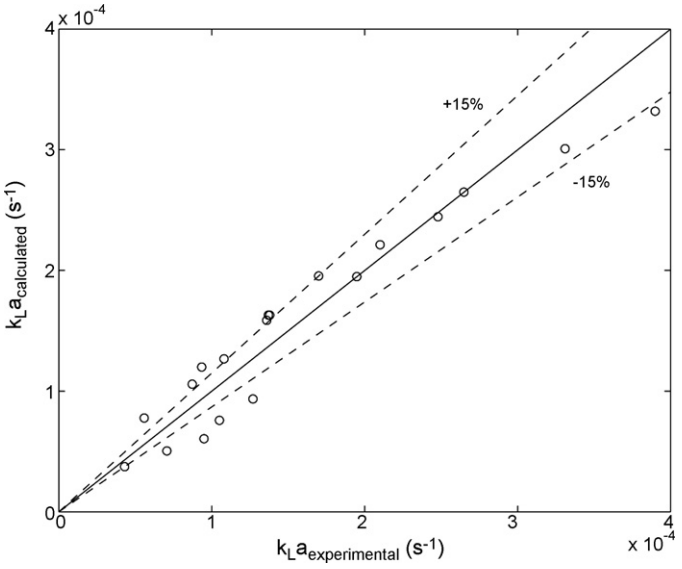

Fig. 2. Comparison between the experimental results obtained using BIOSTAT C® and the fitted ones.

In both Figs. 4 and 5 it can be seen that the experimental k_La turned out to lay within the values predicted by the macromixing mechanism and those predicted by the micromixing mechanism. This was true for all the other impellers (not shown).

Furthermore, there are several considerations to point out. If the impeller is located near the dispersion device, the micromixing is improved in agreement with the results reported by Fournier et al. [11], Lin and Lee [14] and Assirelli et al. [17]. This fact can be due to bubble break up, which modifies the concentration profile surrounding the bubbles during bubble deformation previous to breakage and, once the bubble has broken into parts, the oscillation of the resulting bubbles looking for a stable shape according to its new size also plays an important role on the velocity and concentration profiles defining k_La for each bubble.

In spite of the general conclusion exposed in the previous paragraph, there are cases where the lowest position of the impeller, the closest to the dispersion device, do not improve micromixing. That is the case of the dispersion device of two orifices. This effect can also be seen in Figs. 4 and 5. For this case, the bubbles generated are not big enough to be broken. Therefore, the direct effect of the impellers on the bubbles is smaller and bubble size allows them to follow the flow pattern defined by each impeller. As a result, the location of the impeller does not define k_La since bubble movement across the tank has an important contribution to the total k_La.

The relative position between the impeller and the dispersion device also has a small effect on k_La in case the bubbles generated at the orifices are retained at the impeller's blades for a while before the discharge. Impeller geometry has a lot to do with this fact since the physical effect helps break and disperse the bubbles.

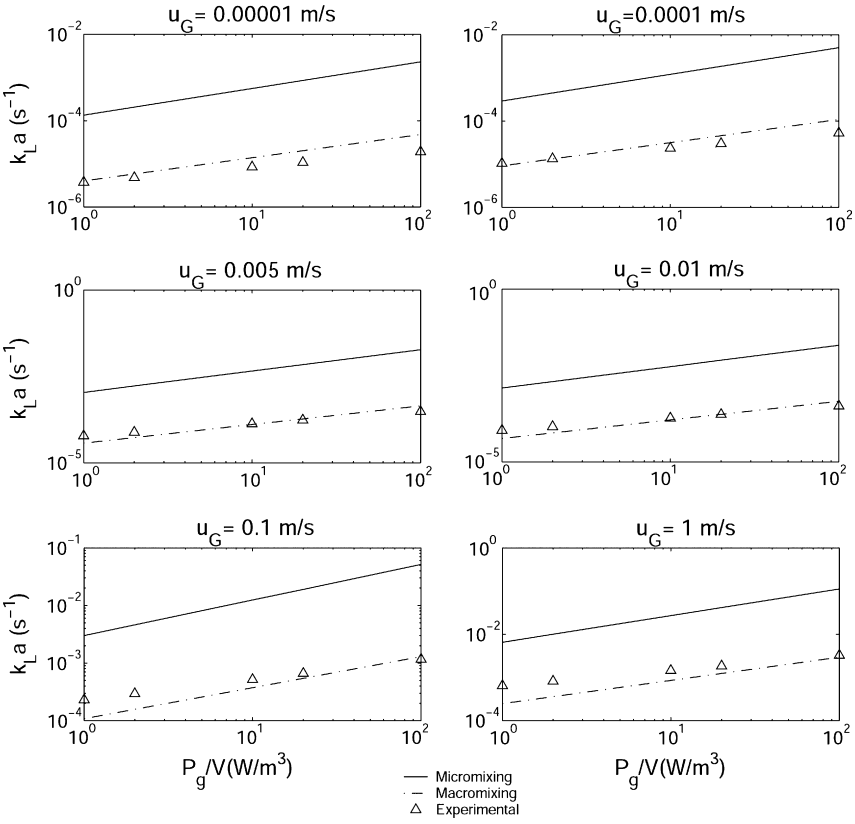

Fig. 3. Effect of the scale up on the contribution of macro and micromixing.

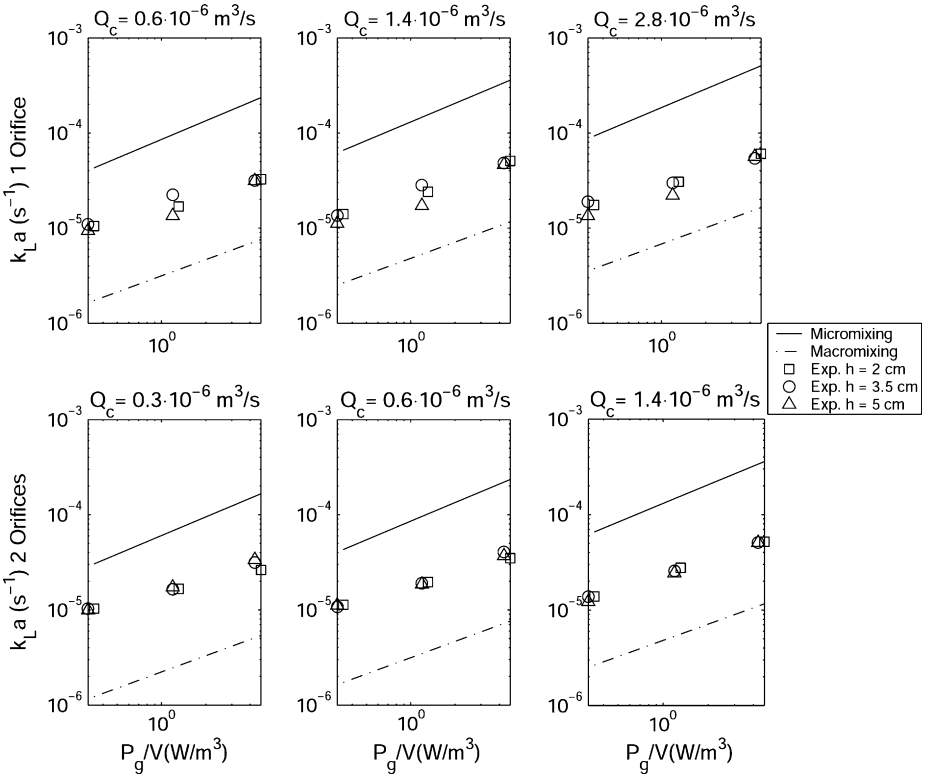

Fig. 4. Effect of the impeller and the dispersion device on the contribution of the macro and micromixing on mass transfer: Rushton turbine.

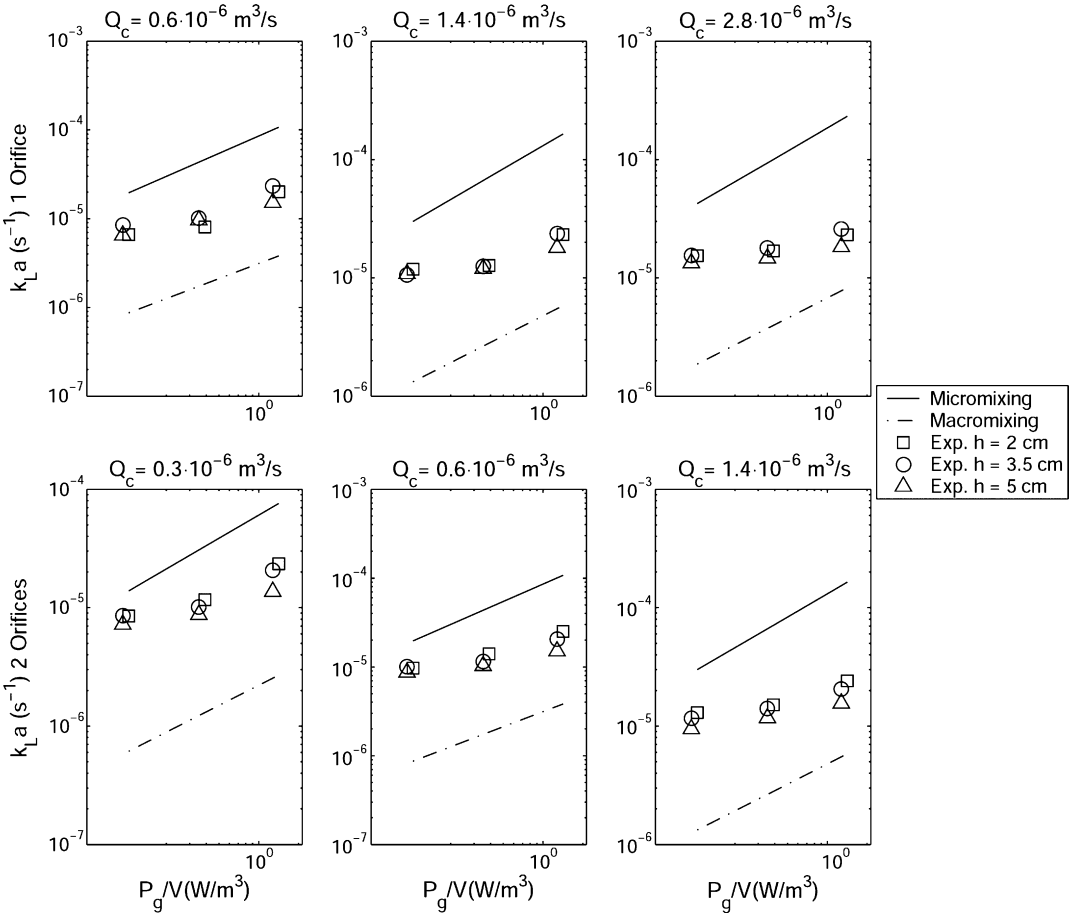

Fig. 5. Effect of the impeller and the dispersion device on the contribution of the macro and micromixing on mass transfer: propeller.

As can be seen in Fig. 12 of a previous work [24], for the case of the Ruston turbine and the Pitched bladed turbine **b**, bubbles are under the influence of the impeller before their breakage and dispersion across the tank. However, for impellers 1 and 2, (pitched blade turbine **a** and a modified blade) the geometry of the blades allows certain bubbles to bypass the impeller.

In order to explain the facts exposed in the previous paragraph, it is important to study the generation of bubble dispersions for the different impellers and the rising paths of the bubbles. The rising path of the bubbles depends on the flow pattern developed for each impeller and it is directly related to the geometry of the blades [24].

In general, $N > 180$ rpm is needed for good dispersions. However, this critical impeller speed depends on the geometry of the blades [24]. In the case of the modified blade (Impeller 2 [24]) N should be bigger than 280 rpm because the anchor type geometry leads the bubbles along preferential paths which makes difficult a good dispersion if radial velocity is not really high. Therefore, if the impeller is located higher, the rising path of the bubbles can lead them away from the blades or parallel to the impeller shaft; so that bubbles bypass the impeller unbroken and tank-sized eddies determine their motion and the gas–liquid contact. Even for bigger impeller speeds, certain big bubbles can avoid the effect of the impeller. This is also the case of impeller 1, a pitched blade turbine with sharp but narrow blades [24]. The blades cannot gather the bubbles which rise in zig-zag due to the flow pattern developed by this impeller and the contribution of the drag and buoyancy forces to the movement of the bubbles. If the bubbles are not cut and/or rise close to the impeller shaft, they will bypass the impeller unbroken. Bubbles can avoid the impeller blades easier if the impeller is located higher. As a result, bubble dispersions are poorer than expected and macromixing plays a bigger role.

For the propeller, the flow field generated reveals a region below the blades of low pressure where bubbles remain, see Fig. 12 Martin et al. [24]. Since bubbles remain there, even for a higher position of the impeller, the effect of the impeller on the bubbles is the same no

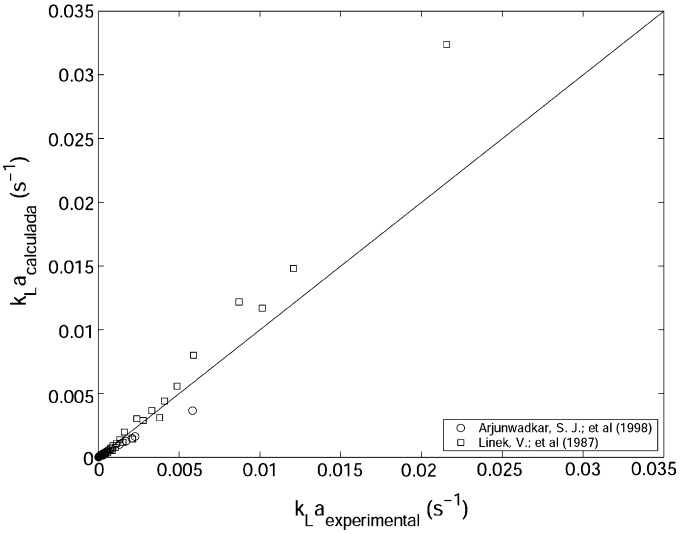

Fig. 6. Combined effect of micro and macromixing on mass transfer for several impeller configurations.

Table 3
Effect of the impeller and the dispersion device on the fraction of the tank where macromixing prevails

Impeller	h (cm)	Perforated plate		Impeller	h (cm)	Perforated plate	
		1 Orifice	2 Orifices			1 Orifice	2 Orifices
1	2	0.61	0.63	4	2	0.46	0.43
	3.5	0.70	0.71		3.5	0.50	0.43
	5	0.75	0.75		5	0.55	0.50
2	2	0.57	0.50	5	2	0.53	0.35
	3.5	0.52	0.55		3.5	0.55	0.37
	5	0.60	0.60		5	0.55	0.40
3	2	0.56	0.50	6 (2 Blades)	2	0.50	–
	3.5	0.60	0.47	6 (3 Blades)	2	0.53	–
	5	0.65	0.50	6 (4 Blades)	2	0.53	–

matter where it is located within the experimental conditions, see Fig. 5. Bubbles are not homogeneously dispersed across the tank. Even though most of these impellers will rarely be used for industrial operation, it is interesting to include them in a comparative study for generate understanding on gas–liquid contact.

Furthermore, if any impeller is located at the highest of the three positions, it is common that the macromixing contribution increases. Bubble motion in the tank and its deformation together with surface aeration have a more important role in k_La, as it can be seen in Figs. 4 and 5. In this case, the removal of the surface of the tank in contact with the atmosphere also increases its contribution to the total k_La. This fact is controlled by the macromixing in the tank too.

The effect of the number of blades on the contribution of the macro and micromixing to k_La has been studied using three impellers, with 2, 3 and 4 blades geometrically identical. It turned out that no clear contribution was obtained. There is an increment in the circulation and the contribution of the surface aeration, that is macromixing contribution but, at the same time, the higher number of blades will also increase the break up and so the micromixing contribution.

In Figs. 1, 3–5, the experimental and empirical results lay within the values predicted by the macro and the micromixing. Therefore, and based on the results exposed by Funahashi et al. [1] and the network of zones models for stirred tanks [30–36], it is possible to define k_La as that given by the contribution of each scale of mixing depending on the region where each of them prevails:

$$\mathrm{Ln}(k_La) = ((1-\chi)\mathrm{Ln}(k_La_{\mathrm{Micromixing}}) + (\chi)\mathrm{Ln}(k_La_{\mathrm{Macromixing}})) \quad (14)$$

χ is defined as the fraction of the tank where macromixing prevails and depends on the type of impeller or impellers and the internal configuration of the tank [1,15,17].

Eq. (14) is able to fit the experimental results with the effects of the macro and micromixing on the mass transfer for Linek et al. [53] and Arjunwadkar et al. [54], with χ equal to 0.72 and 0.12, respectively. Fig. 6 shows the comparison between the experimen-

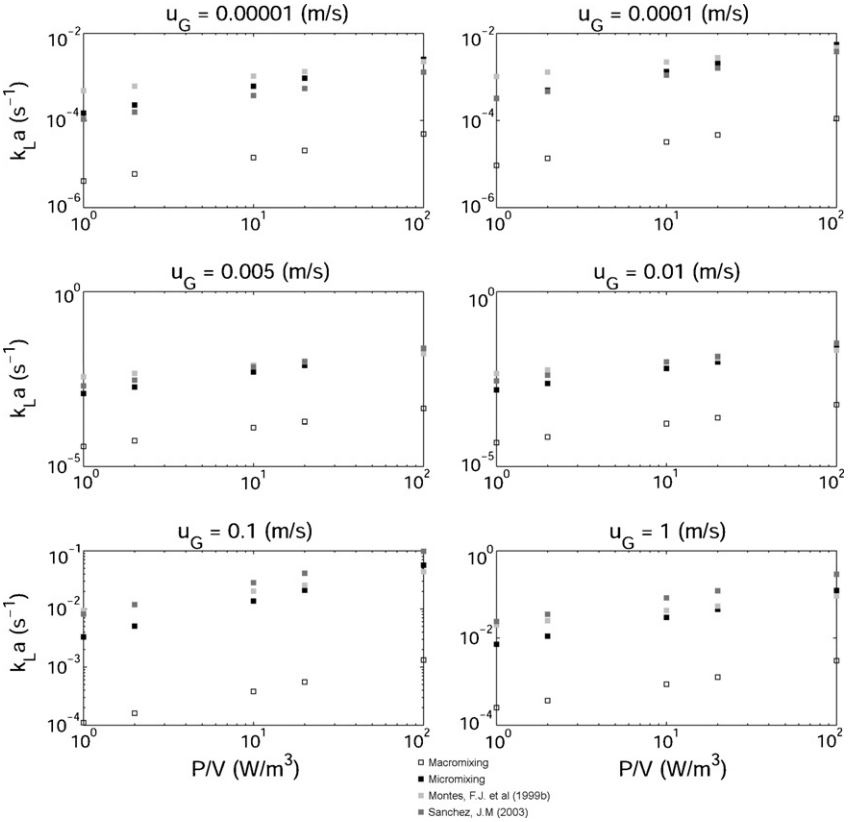

Fig. 7. Macro and micromixing effects in a system with oxygen consumption.

Table 4
Volumetric mass transport coefficients under oxygen consumption conditions

	k	α	β	Operating conditions	Impeller type
[59]	8.8×10^{-2}	0.4	0.46	BIOSTAT C®	3 Rushton turbines
[60]	2.4×10^{-2}	0.54	0.47		

tal values of k_La and those obtained using Eq. (14). Good agreement is found using the calculated values of χ. In case of the data from BIOSTAT C®, Fig. 3, χ was equal to 1.

In Table 3 the results of χ from fitting the experimental results obtained using the non standard tank [58] to Eq. (14) are shown.

The above exposed conclusions regarding the effect of the bubble size and impeller (blade geometry and position) on the contribution of macro and micromixing on k_La can be also obtained from the analysis of the fitting coefficients seen in Table 3.

If there is consumption of oxygen in the bulk phase, the enhancement in mass transfer increases the value of the proportional constant in the empirical equations for k_La, [27].

Montes et al. [59] and Sánchez [60] studied the mass transfer rates during the growth of *Trigonopsis Variabilis* and *Bacilus Licheniformis* respectively using a BIOSTAT C®. The empirical fitting coefficients of the experimental data to Eq. (12) can be seen in Table 4.

If a figure in the form of 1 or 3 is prepared using the experimental data form Montes et al. [59] and Sánchez [60], Fig. 7, it can be seen that the experimental k_La values are close to the ones predicted by the micromixing mechanism. The consumption of oxygen by the media increases the measured k_La since the equilibrium in the gas–liquid interphase has been displaced as oxygen disappears consumed in the liquid phase. That consumption increases the concentration gradients surrounding the bubbles and so, enhances mass transfer. The concentration gradients surrounding the bubbles depend on the kinetics of the reaction. In order to explain and model the effect of a chemical reaction in the tank, an enhancement factor has traditionally been included multiplying the total k_La [25].

If the values of k_La are fitted to Eq. (14) the χ is 0 and 0.003 for the Montes et al. [59] and Sánchez [60] results respectively.

Comparing Figs. 1 and 7, it can be concluded that, apart from the differences in the liquid phase, the consumption of oxygen increases the term related to the liquid film resistance as an enhancement factor [27]. Therefore, it can be considered that both contributions (that of micromixing and that of macromixing) are enhanced. Furthermore, micromixing cannot explain the effect of the geometry of the system, which is one of the problems in equipment scale up.

5. Conclusions

Mass transfer in stirred tanks can be explained by coupling the effects of the two most important scales of mixing inside it, the micromixing scale and the macromixing scale. Each mixing scale has a particular effect on the mass transfer rate.

Macromixing accounts for the geometrical configuration of the reactor, where the scaled up problems are focused. It determines the deformation of the bubbles and its path across the reactor as well as the contribution of the surface aeration.

Micromixing takes into consideration the small eddies responsible for the concentration gradients surrounding. Bubble break up increases the contribution of the micromixing scale to the total k_La.

In absence of consumption of gas in the liquid phase, both mechanisms are important. However, the enhancement in the mass transfer due to the consumption of oxygen in the media results in mass transfer values close to those given by the micromixing mechanisms.

Using the scale up strategy based on constant power input reduces the impeller speed. According to the results shown, this strategy increases the contribution of the macromixing to k_La.

Acknowledgments

The support of the Ministerio de Educación y Ciencia of Spain providing a F.P.U. fellowship to M. Martín is greatly welcomed. The funds from the project reference CTQ 2005–01395/PPQ are also appreciated.

References

[1] H. Funahashi, K.I. Hirai, T. Yoshida, H. Taguchi, Mechanistic analysis of xathan gum production in a stirred tank, J. Ferment. Technol. 66 (3) (1988) 355–364.
[2] K. Kling, D. Mewes, Two-colour laser induced fluorescence for the quantification of micro- and macromixing in stirred vessels, Chem. Eng. Sci. 59 (2004) 1523–1528.
[3] J. Baldyga, J.R. Bourne, S.J. Hearn, Interaction between chemical reactions and mixing on various scales, Chem. Eng. Sci. 52 (4) (1997) 457–466.
[4] M. Buchmann, D. Mewes, Tomographic measurements of micro- and macromixing using the dual wavelength photometry, Chem. Eng. J. 77 (1–2) (2000), 3–9.
[5] A.W. Nienow, S.M. Drain, A.P. Boyes, K.J. Carpenter, An experimental study to characterize imperfect macromixing in a stirred semibatch reactor, Ind. Eng. Chem. Res. 36 (1997) 2984–2989.
[6] A.W. Nienow, S.M. Drain, A.P. Boyes, R. Mann, A.M. El-Hamouz, K.J. Carpenter, A new pair of reactions to characterize imperfect macro-mixing and partial segregation in a stirred semi-batch reactor, Chem. Eng. Sci. 47 (9–11) (1992), 2825–2830.
[7] K. Kling, D. Mewes, Two-colour laser induced fluorescence for the quantification of micro- and macromixing in stirred vessels, Chem. Eng. Sci. 59 (7) (2004) 1523–1528.
[8] P.E. Arratia, J.P. Lacombe, T. Shinbrot, F.J. Muzzio, Segregated regions in continuous laminar stirred tank reactors, Chem. Eng. Sci. 59 (2004) 1481–1490.
[9] M. Zlokarnik, Scale-up in Chemical Engineering, Wiley VCH, Weinheim, 2002.
[10] J. Kilander, S. Blomstrom, A. Rasmuson, Scale up behaviour in stirred square floculation tanks, Chem. Eng. Sci. 62 (2007) 1606–1618.
[11] M.C. Fournier, L. Falk, J. Villermaux, A new parallel competing reaction system for assessing micromixing efficiency – determination of micromixing time by a simple mixing model, Chem. Eng. Sci. 51 (23) (1996) 5187–5192.
[12] M. Rahimi, R. Mann, Macro-mixing, partial segregation and 3-D selectivity fields inside a semi-batch stirred reactor, Chem. Eng. Sci. 56 (2001) 763–769.
[13] R. Mann, A. Togatorop, P.R. Senior, P. Graham, B. Edwards, Evaluating mixing in stirred reactors by 3-D visualization: partial segregation for dual-feed semi-batch operation, Chem. Eng. Res. Des. 75 (November (8)) (1997) 755–762.
[14] W.W. Lin, D.J. Lee, Micromixing effects in aerated stirred tank, Chem. Eng. Sci. 52 (21–22) (1997) 3837–3842.
[15] A. Amanullah, L. Serrano-Carreon, B. Castro, E. Galindo, A.W. Nienow, The influence of impeller type in pilot scale xanthan fermentations, Biotech. Bioeng. 57 (1) (1997) 95–108.
[16] D. Vlaev, R. Mann, V. Lossev, S.D. Vlaev, J. Zahradnik, P. Seichter, Macro-mixing and streptomyces fradiae: modelling oxygen and nutrient segregation in an industrial bioreactor, Chem. Eng. Res. Des. 78 (3) (2000) 354–362.
[17] M. Assirelli, W. Bujalski, A. Eaglesham, A.W. Nienow, Study of micromixing in a stirred tank using a Rushton turbine—Comparison of feed positions and other mixing devices, Chem. Eng. Res. Des. 80 (8) (2002) 855–863.
[18] F.J. Montes, M.A. Galán, R.L. Cerro, Mass transfer from oscillating bubbles in bioreactors, Chem. Eng. Sci. 54 (1999) 3127–3136.
[19] A.W. Nienow, On impeller circulation and mixing effectiveness in the turbulent flow regime, Chem. Eng. Sci. 52 (15) (1997) 2557–2565.
[20] Y. Kawase, M. Moo-Young, Volumetric mass transfer coefficients in aerated stirred tank reactors with Newtonian and non Newtonian media, Chem. Eng. Res. Des. 66 (1988) 284–288.
[21] F. García Ochoa, E. Gómez, Theoretical prediction of gas–liquid mass transfer coefficient, specific area and hold up in sparger stirred tanks, Chem. Eng. Sci. 59 (2004) 2489–2501.
[22] G.A. Hugmark, Power requirements and interfacial area in gas–liquid turbine agitated systems, Ind. Eng. Chem. Proc. Des. Dev. 19 (1980) 638–641.
[23] V.B. Shukla, U.P. Veera, P.R. Kulkarni, A.B. Pandit, Scale up of biotransformation process in stirred tank reactor using dual impeller bioreactor, Biochem. Eng. J. 8 (2001) 19–29.
[24] M. Martin, F.J. Montes, M.A. Galán, Bubbling process in stirred tank reactors I: Agitator effect on bubble size, formation and rising, Chem. Eng. Sci. 63 (2008) 3212–3222.
[25] W.-M. Lu, H.-Z. Wu, M.-Y. Ju, Effects of baffle design on the liquid mixing in an aerated stirred tank with standard Rushton turbine impellers, Chem. Eng. Sci. 52 (21–22) (1997) 3843–3851.

[26] P.R. Gogate, A.A.C.M. Beenackers, A.B. Pandit, Multiple-impeller systems with a special emphasis on bioreactors: a critical review, Biochem. Eng. J. 6 (2000) 109–144.
[27] K. Terasaka, J. Oka, H. Tsuge, Ammonia absorption from a bubble expanding at a submerged orifice into water, Chem. Eng. Sci. 57 (18) (2002) 3757–3765.
[28] P.V. Dankwerts, B.E. Kennedy, Kinetics of liquid-film process in gas absorption. Part I: Models of the absorption process, Trans. IChemE 32 (1954) S49–S52.
[29] J. Cheng, Z.R. Yang, H.Q. Chen, C.H. Kuo, M.E. Zappi, Simultaneous prediction of chemical mass transfer coefficients and rates for removal of organic pollutants in ozone absorption in an agitated semi-batch reactor, Sep. Purif. Tech. 31 (2003) 97–104.
[30] P. Vrabel, R.G.J.M. van der Lans, K.C.A.M. Luyben, L. Boon, A.W. Nienow, Mixing in large-scale vessels stirred with multiple radial or radial and axial up-pumping impellers: modelling and measurements, Chem. Eng. Sci. 55 (2000) 5881–5896.
[31] S.S. Alves, J.M.T. Vasconcelos, J. Barata, Alternative compartment models of mixing in tall tanks agitated by multi-rushton turbines, Chem. Eng. Res. Des. 75 (Part A) (1997) 334–338.
[32] J.M.T. Vasconcelos, S.S. Alves, J.M. Barata, Mixing in gas–liquid contactors agitated by multiple turbines, Chem. Eng. Sci. 50 (14) (1995) 2343–2354.
[33] R. Mann, Gas–liquid stirred vessel mixers: towards a unified theory based on network of zones, Trans. Inst. Chem. Engrs. 37 (1986) 23–34.
[34] H. Alexopoulos, D. Maggioris, C. Kiparissides, CFD analysis of turbulence non-homogeneity in mixing vessels: A two-compartment model, Chem. Eng. Sci. 57 (10) (2002) 1735–1752A.
[35] H. Hristov, R. Mann, V. Lossev, S.D. Vlaev, P. Seichter, A 3-D analysis of gas-liquid mixing, mass transfer and bioreaction in a stirred bio-reactor, Food Bioprod. Process. 79 (4) (2001) 232–241.
[36] J. Zahradník, R. Mann, M. Fialová, D. Vlaev, S.D. Vlaev, V. Lossev, P. Seichter, A networks-of-zones analysis of mixing and mass transfer in three industrial bioreactors, Chem. Eng. Sci. 56 (2) (2001) 485–492.
[37] V.M. Barabash, M.A. Belevitskaya, Mass transfer from bubbles and crops in mechanically agitated apparatuses, Theor. Found. Chem. Eng. 29 (4) (1995) 333–342.
[38] R. Higbie, The rate of absorption of a pure gas into a still liquid during a short time of exposure, Trans. Am. Inst. Chem. Eng. 31 (1935) 365–389.
[39] P.H. Calderbank, Physical rate processes in industrial fermentation: Part I "The interfacial area in gas liquid contacting with mechanical agitation", Trans. Inst. Chem. Engrs. 37 (1958) 443–463.
[40] P.V. Dankwerts, Significance of liquid-film coefficients in gas absorption, Ind. Eng. Chem. 43 (1951) 1460–1467.
[41] S. Ruszkowski, A rational method for measuring blending performance and comparison of different impeller types, in: Proc. Eighth European Mix. Conf., Inst. Chem. Eng., Rugby, UK, 1994, pp. 283–291.
[42] R.K. Grenville, S. Ruszkowski, E. Garred, Blending of miscible liquids in the turbulent and transitional regimes, in: 15th NAMF Mixing Conference 1995, Banff, Canada, 1995.
[43] D. Pinelli, A. Bakker, K.J. Myers, M.F. Reeder, J. Fasano, F. Magelli, Some features of a novel gas dispersion impeller in a dual-impeller configuration, Chem. Eng. Res. Des. 81 (4) (2003) 448–454.
[44] G. Fabrice, T. Christian, Mixing in industrial Rushton turbine-agitated reactors under aerated conditions, Chem. Eng. Process. 42 (2003) 373–386.
[45] M. Cooke, J.C. Middleton, J.R. Bush, Mixing and mass transfer in filamentous fermentations, in: Proceedings of the 2nd International Conference on Bioreactor Fluid Dynamics, BHRA, Cranfield, UK, 1988, pp. 37–64.
[46] S. Hiraoka, Y. Kato, Y. Tada, N. Ozaki, Y. Murakami, Y.S. Lee, Power consumption and mixing time in an agitated vessel with double impeller, Chem. Eng. Res. Des. 79 (8) (2001) 805–810.
[47] D.J. Groen, Macromixing in bioreactors, Ph.D. thesis, Delft University of Technology, The Netherlands, 1994.
[48] D. Hadjiev, N.E. Sabiri, A. Zanati, Mixing time in bioreactors under aerated conditions, Biochem. Eng. J. 27 (2006) 323–330.
[49] E. Ruckenstein, Mass transfer in the case of interfacial turbulence induced by the Marangoni effect, Int. J. Heat Mass Transfer 11 (1968) 1753–1760.
[50] A. Sethy, H.T. Cullinan, Transport of mass in liquid–liquid systems. Part II: Mass transfer and interfacial studies, AIChE J. 21 (3) (1975) 575–582.
[51] M. Tourneau, S. Wolf, J. Stichlmair, Influence of interfacial convections on mass transfer in liquid–liquid systems at plane interfaces, Transport mechanisms across Fluid Interfaces, DECHEMA Monographs, vol. 136, Wiley-VCH, Weinheim, Monographie, 2000.
[52] I.W. Richards, Power input to fermenters and similar vessels, Br. Chem. Eng. 8 (1963) 158–163.
[53] V. Linek, V. Vacek, P. Benes, A critical review and experimental verification of correct use of dynamic method for the determination of oxygen transfer in aerated agitated vessels to water, electrolytic solutions and viscous liquids, Chem. Eng. J. 34 (1987) 11–34.
[54] S.J. Arjunwadkar, K. Sarvanan, A.B. Pandit, P.R. Kulkarni, Gas liquid mass transfer in dual impeller bioreactor, Biochem. Eng. J. 1 (1998) 99–106.
[55] C.O. Vandu, R. Krishna, Influence of scale on the volumetric mass transfer coefficients in bubble columns, Chem. Eng. Process. 43 (2004) 575–579.
[56] N.D.P. Dang, D.A. Karrer, I.J. Dunn, Oxygen transfer coefficients by dynamic model moment analysis, Biotechnol. Bioeng. 19 (1977) 853–865.
[57] K. Van't Riet, Review of measuring methods and results in non viscous gas liquid mass transfer in stirred vessels, Ind. Eng. Chem. Proc. Dev. 18 (1979) 357–364.
[58] M. Martín, F.J. Montes, M.A. Galán, Bubbling Process in stirred tank reactors II: agitator effect on mass transfer, Chem. Eng. Sci. 63 (2008) 3223–3234.
[59] F.J. Montes, J. Catalán, M.A. Galán, Prediction of k_La in yeast broths, Process Biochem. 34 (1999) 549–555.
[60] J.M. Sánchez, Caracterización y desarrollo del enriado biotecnológico para la extracción de fibras del lino, PhD Thesis, Univ. Salamanca, 2003.
[61] J.H. Rushton, E.W. Costich, H.J. Everett, Power characteristics of mixing impellers, part II, Chem. Eng. Prog. 46 (9) (1950) 467–476.
[62] R.J. Weetman, J.Y. Oldshue, Comparison of Mass Transfer Characteristics of Radial and Axial Flow Impellers 6th European Conference on Mixing, Pavia, Italy, ISBN 0 947711 33 3, May 24–26, 1988.